

# Eksploatacja i Niezawodnosc – Maintenance and Reliability Volume 28 (2026), Issue 1

journal homepage: http://www.ein.org.pl

Article citation info:

Gładysz P, Merkisz J, Borucka A, Reliability of Unmanned Aerial Vehicles in the Context of Selected Factors, Eksploatacja i Niezawodnosc – Maintenance and Reliability 2026: 28(1) http://doi.org/10.17531/ein/210312

# Reliability of Unmanned Aerial Vehicles in the Context of Selected Factors



## Piotr Gładysz<sup>a,\*</sup>, Jerzy Merkisz<sup>a</sup>, Anna Borucka<sup>b</sup>

- <sup>a</sup> Poznan University of Technology, Poland
- <sup>b</sup> Military University of Technology, Poland

### Highlights

- There is a relationship between the type of failure and the time of its occurrence.
- Bad weather conditions affect the time of UAV failure.
- Type of failure and the time of its occurrence is information useful in operating the UAV.

This is an open access article under the CC BY license (https://creativecommons.org/licenses/by/4.0/)

#### **Abstract**

This article focuses on the study of the reliability of unmanned aerial vehicles (UAVs), whose role in various sectors, including the rescue sector, is dynamically increasing. The aim of the study was to analyze the key factors affecting UAV failure rate and determine their impact on the time to failure. Statistical analysis and simulations were conducted within the study, based on collected data, to investigate the relationship between the type of failure and the system's time to failure. The results of the analyses showed that the time to failure differs significantly depending on the cause, particularly for battery-related failures. It was also found that unfavorable atmospheric conditions, such as strong wind, high temperature, and high humidity, significantly shorten the system's time to failure compared to normal conditions, with this effect being similar for different types of unfavorable weather.

#### Keywords

energy consumption, battery, UAV, energy management

#### 1. Introduction

Research on the failure rates of unmanned aerial vehicles (UAVs) has gained particular significance with the rapid increase in their use across civil, commercial, and military sectors [4, 5]. One of the key factors associated with the development of this technology is ensuring the stability, duration, and safety of operations, thus ensuring smooth integration with airspace. The literature on the subject highlights several factors that influence drone failure rates, which can be categorized into three main groups: technical factors [8, 9], environmental factors [11, 12], and those related to human error [6, 7, 10]. Each of these categories represents a different source of risks and potential malfunctions that may lead to failure or directly to an accident involving unmanned

aerial vehicles [1].

Technical factors primarily include design defects, component wear, software malfunctions, and power supply issues [17, 18]. Examples of such issues include engine failures [14], propeller problems [13], control system malfunctions, battery failures, or communication system problems [23]. A frequent source of issues are also software errors, including those resulting from incorrect coding as well as lack of updates to operating systems or controlling applications [19, 20]. Furthermore, poor quality of materials used and improper maintenance of the aircraft can significantly increase the risk of technical failure [15, 16], especially in situations when commercial UAVs are used in rescue and crisis operations.

(\*) Corresponding author.

E-mail addresses:

P. Gładysz (ORCID: 0000-0002-4676-2006) phddron@gmail.com, J. Merkisz (ORCID: 0000-0002-1389-0503) jerzy.merkisz@put.poznan.pl, A. Borucka (ORCID: 0000-0002-7892-9640) anna.borucka@wat.edu.pl,

Eksploatacja i Niezawodność - Maintenance and Reliability Vol. 28, No. 1, 2026

Another group consists of environmental factors, which stem from the conditions in which unmanned aerial vehicles conduct flights. These include, among others, adverse weather and climatic conditions such as strong winds, rainfall, snowfall, fog, or fluctuating temperatures, as well as lightning strikes [2, 21, 22]. The presence of terrain obstacles, such as trees, power lines, or tall buildings, also increases the risk of collisions and equipment damage [23, 24]. Additionally, GPS signal interference or electromagnetic disturbances, occurring for example near large industrial installations, may result in a loss of control over the device [25, 26]. Another significant factor posing a threat during UAV operations is hacking and unauthorized pairing. Such activities may lead to the takeover of control over the drone, data theft, or disruption of its mission. Therefore, it is crucial to implement advanced cybersecurity measures, such as strong encryption and access control, in order to protect drones from unauthorized integration and ensure the continuity of safe aerial operations [43].

Equally important are factors related to human error [6, 7, 10]. The literature emphasizes that insufficient operator training, improper mission planning, misjudgment of the situation, or non-compliance with operational procedures are among the main causes of failures and accidents [27, 28]. It often occurs that drone operators overestimate the capabilities of the disregard limitations equipment or resulting from environmental conditions, which leads to dangerous situations. Additionally, errors in system configuration, improper control, or failure to respond to warning signals from the system may contribute to uncontrolled events. It should also be emphasized that flying in crisis situations is characterized by a significant psychophysical load. Pilots conducting flights during rescue operations must deal with time pressure, fatigue, noise, light flashes, and extremely risky flight maneuvers.

Thus, the failure rate of unmanned aerial vehicles is a complex and multifactorial phenomenon. Understanding and identifying the sources of potential threats – both technical, environmental, and those arising from human error – is crucial for improving the safety of operations involving unmanned aerial vehicles. A proper analysis of these factors enables the development of effective strategies for minimizing failure risks and enhancing the overall reliability of drone systems.

Therefore, failure analysis is a frequently addressed topic in

scientific publications. Many studies utilize a statistical approach. For instance, NTSB reports and the Aviation Safety Reporting System (ASRS) database are often sources of empirical data for regression analysis and hazard modeling, which help determine the probability of failure depending on flight time, weather conditions, or mission type [29, 30]. In works such as those by Clothier et al. [31], probabilistic models have been developed to predict the consequences of failures in the context of threats to people and infrastructure. Another commonly used research method is computer simulations [34] and numerical analyses [35], particularly in assessing the reliability of unmanned systems. Works by Ghazali et al. [32] and Iannace et al. [33] utilize artificial intelligence for fault detection. These studies have shown that the integration of diagnostic systems based on machine learning can significantly enhance UAVs' ability to identify and compensate for malfunctions in real-time. In [13], the authors proposed using a clustering algorithm -k-means - to detect UAV failures during flight, focusing particularly on propeller malfunctions and failures. Field studies are also being conducted. Authors such as Salazar et al. [36, 37] have analyzed real-world cases of drone failures used in logistics and environmental monitoring. They demonstrated that the most common causes of failures are power issues (e.g., battery failures), communication disruptions, and software errors. The significant impact of weather conditions, especially wind and precipitation, on the reliability of UAV systems is also highlighted [41, 42].

In summary, the literature on drone failure rates covers a broad range of research methods, from statistical analysis and risk modeling, to computer simulations, empirical studies, and applications in real-world flight conditions. The results of these studies not only provide insights into the most frequent causes of malfunctions but also suggest directions for further development of technologies that enhance flight safety, such as autonomous diagnostic systems, system redundancy, and improved route planning algorithms that take risks into account.

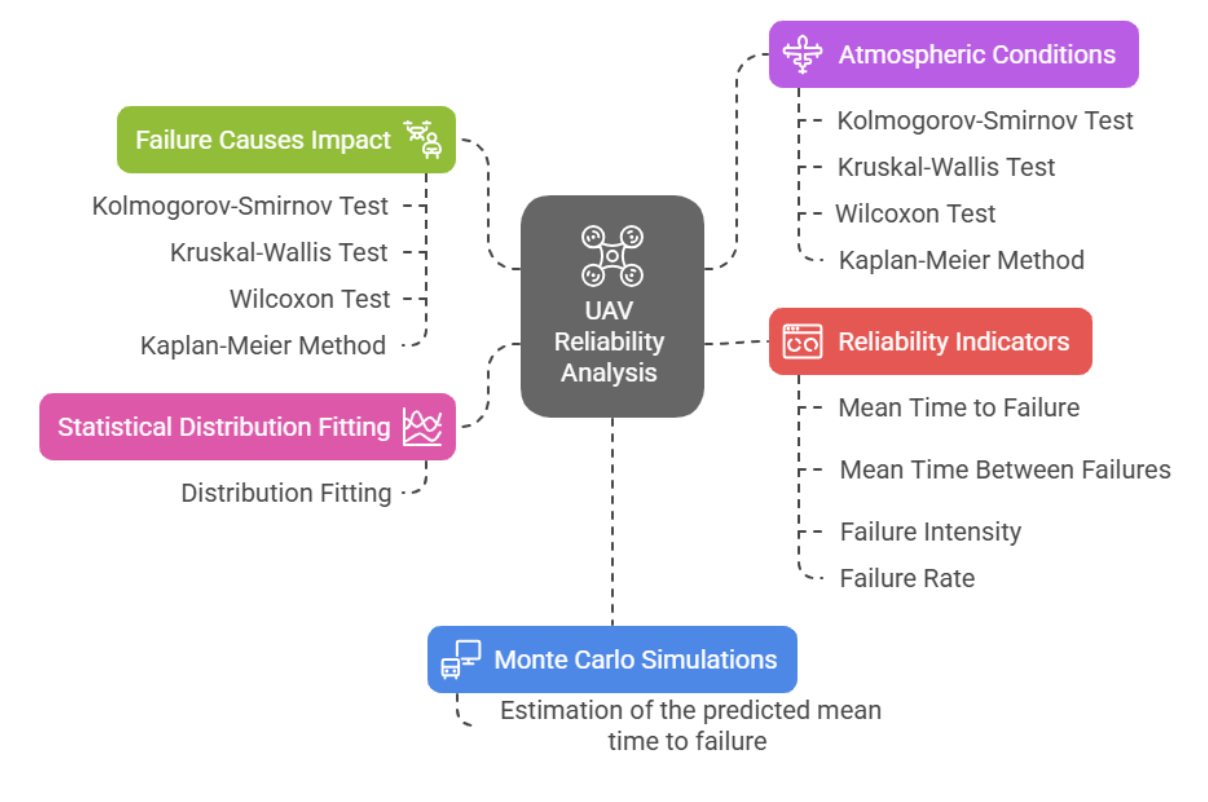
Overall, it can be stated that research on drone failure rates focuses on several key areas, including the identification of factors affecting the reliability of these devices, the development of methods for assessing their reliability, and the evaluation of the effectiveness of different approaches in minimizing failure risks.

This article presents an analysis and evaluation of the causes of battery failures in unmanned aerial vehicles used by the State and Volunteer Fire Departments, as well as a study of the distribution of time to failure using the Weibull distribution model. The application of this approach allowed for a detailed assessment of the characteristics and dynamics of damage under specific conditions of intensive operation. The unique nature of this work lies in the inclusion of real-world data from rescue systems, which has been rarely studied so far. This analysis not only allows for a better understanding of failure mechanisms but also enables the forecasting of battery lifespan under high-risk operational conditions. The results obtained may provide a significant contribution to the development of reliability management methods for equipment used in emergency services.

#### 2. Material and methods

#### 2.1. Algorithm for the Study

The study utilized data provided by pilots from the State and Volunteer Fire Departments regarding the operation of unmanned aerial vehicles (UAVs) collected during training and operational flights conducted by fire protection units. The entire aerial operation was carried out using an electrically powered quadcopter with two LiPo batteries. Based on the reports, databases were created containing information on the UAV's non-failure operation time, which is the dependent variable in this study, the cause of failure, and additionally describing the existing weather conditions that may have influenced the occurrence of the malfunction (high temperature, strong wind, humidity). The study was conducted according to the algorithm presented in Figure 1.



Made with ≽ Napkin

Figure 1. Research Procedure Algorithm

According to the presented scheme, the first step involved characterizing and assessing the impact of selected factors on the non-failure operation time of unmanned aerial vehicles (UAVs). To verify the normality of the distribution, the Kolmogorov-Smirnov test was used [39, 40]. The Kolmogorov-

Smirnov test utilizes the distance between the empirical cumulative distribution function and the theoretical normal distribution  $N(\mu, \sigma^2)$ . It should be applied to a large number of samples. If the parameters of the distribution are not known, the estimators of the mean value  $\mu$  and standard deviation  $\sigma$  are

determined on a sample basis. For an ordered realization of the sample  $x_{(1)} \le x_{(2)} \le ... \le x_{(n)}$  we define an empirical distribution of the form:

$$F_n(x) = \begin{cases} 0, & dla \ x < x_{(1)}, \\ \frac{i}{n}, & for \ x_{(i)} \le x < x_{(i+1)}, 1 \le i < n, \\ 1, & dla \ x \ge x_{(n)}. \end{cases}$$

The theoretical distribution of a normal distribution is expressed by the formula:

$$F(x) = \int_{-\infty}^{x} \frac{1}{\sqrt{2\pi}\sigma} e^{-\frac{(s-\mu)^2}{2\sigma^2}} ds,$$

The value of the test statistic  $D_n$  is determined as:

$$D_n = \max_{1 \le i \le n} |F_n(x_{(i)}) - F(x_{(i)})|.$$

The  $D_n$  test statistic has a Kolmogorov-Smirnov distribution. For a given significance level  $\alpha$ , if the test probability value p satisfies the condition  $p < \alpha$ , then the null hypothesis  $H_0$  is rejected in favor of the alternative hypothesis  $H_1$ .

The impact of individual causes of UAV failure on the non-failure operation time was assessed using the non-parametric Kruskal–Wallis test [38]. In the Kruskal–Wallis test, for the studied variable X, a sample is taken for k groups. Let  $x_i = \{x_{i1}, x_{i2}, ..., x_{i,n_i}\}$  denote the realization for i-th group and i = 1,2,...,k, while let  $F_i(x)$  denote the distribution for i-th group. A working hypothesis is created at the significance level  $0 < \alpha < 1$ :

 $H_0$ :  $F_1(x) = F_2(x) = \dots = F_k(x)$  – the distributions within the groups are identical or differ insignificantly (no differences between the effects),

against the alternative hypothesis:

 $H_1$  – there are such i, j that  $F_i(x) \neq F_j(x)$  – distributions within the groups differ significantly.

To verify these hypotheses, we first perform rankings for the entire sample

$$\left\{x_{11}, x_{12}, \ldots, x_{1,n1}, x_{21}, x_{22}, \ldots, x_{2,n2}, x_{31}, x_{32}, \ldots, x_{k,n_k}\right\}$$

 $R_{ij}$  denotes the rank for the element  $x_{ij}$ ,  $1 \le i \le k$ ,  $1 \le j \le n_i$ . Each group  $X_i$  corresponds to a sequence of ranks  $R_i = \{R_{i1}, R_{i2}, ..., R_{i,n_i}\}$ , for which we determine the average rank for i-th group:

$$\overline{R}_i = \frac{1}{n_i} \sum_{j=1}^{n_i} R_{ij}.$$

The test statistic is given by the formula:

$$KW = \frac{12}{n(n+1)} \sum_{i=1}^{k} n_i \left( \overline{R}_i - \frac{n+1}{2} \right)^2$$

and it is a measure of the deviation of the sample mean ranks from  $\frac{n+1}{2}$ . The test statistic KW follows  $\chi^2$  distribution with (k-1) degrees of freedom. At a given significance level  $\alpha$ , if  $p < \alpha$ , there is sufficient evidence to reject the null hypothesis  $H_0$  in favor of the alternative hypothesis, which means that at least one of the compared groups differs significantly from the others. A post-hoc analysis, aimed at examining the significance of differences between individual pairs of failure causes, was carried out using the Wilcoxon test with adjusted p values. The test examines the difference between the paired values of the studied characteristic  $d_i = x_{i1} - x_{i2}$  for i = 1, 2, ..., n tested objects. This difference is used to verify the hypothesis that the median of the differences is 0,

$$H_0: M_e = 0$$

against the alternative hypothesis that the median is different from zero:

$$H_1: M_e \neq 0$$
,

The test statistic is calculated using the absolute values  $|d_i|$ , i = 1, ..., n and the sum of ranks for each group in the form:

$$T_{-} = \sum_{d_i < 0} R_i$$
,  $T_{+} = \sum_{d_i > 0} R_i$ .

For  $n\to\infty$ , the statistic  $T_+$  follows the distribution  $N\left(\frac{n(n+1)}{4},\frac{n(n+1)(2n+1)}{24}\right),$ 

while the statistic:

$$Z = \frac{T_{+} - \frac{n(n+1)}{4}}{\sqrt{\frac{n(n+1)(2n+1)}{24}}},$$

follows the distribution N(0,1). The critical area is of the form:

$$W = (-\infty, -u_{1-\frac{\alpha}{2}}] \cup \left[-u_{1-\frac{\alpha}{2}}, +\infty\right).$$

If  $Z \in W$ , then at the significance level  $\alpha = 0.05$ , we reject the null hypothesis  $H_0$  in favor of the alternative hypothesis  $H_1$ .

To precisely examine and compare the impact of individual factors on the time to failure, the Kaplan-Meier survival analysis method was applied. This method is particularly useful in analyzing the time until an event occurs (in this case – a failure), allowing for the inclusion of censored observations,

meaning those cases where a failure did not occur during the observation period. Thanks to the use of the Kaplan-Meier analysis, it was also possible to determine the survival function separately for each of the analyzed groups of failure-causing factors. The Kaplan-Meier estimator describes the probability of survival (i.e., no failure) beyond a certain time t and is expressed by the formula:

$$\hat{S}(t) = \prod_{t_i \le t} \left( 1 - \frac{d_i}{n_i} \right)$$

where  $t_i$  - the moment the next failure occurs,  $d_i$  - the number of failures over time,  $n_i$  - the number of elements 'surviving' just before time.

A visual comparison of the survival curves between groups was presented using survival plots, which enables quick identification of factors associated with a faster occurrence of failures. To additionally verify the statistical significance of differences between groups, the log-rank test was used. The test statistic is expressed by the formula:

$$Q = \frac{\left(\sum_{i=1}^{k} (O_i - E_i)\right)^2}{\sum_{i=1}^{k} V_i}$$

where:  $O_i$  - the number of observed events (failures) in the i group,  $E_i$  - the expected number of events in the i group assuming equality of the survival function,  $V_i$  - the variance for the igroup, k - the number of groups compared. The statistic Q follows a chi-square distribution ( $\chi^2$ ) with k-1 degrees of freedom. If the value  $p < \alpha$ , we reject the null hypothesis, which assumes identical survival functions across all groups.

The next part of the study concerns the reliability assessment of the analyzed UAV. In the first stage, appropriate statistical distributions were fitted to the empirical data, which allowed for further reliability modeling. For this purpose, the Maximum Likelihood Estimation (MLE) method was used, and the following distributions were proposed: Weibull, exponential,

log-normal, and gamma. After fitting the statistical distribution, a Monte Carlo simulation was conducted to estimate the predicted mean time to UAV failure.

The study went on to calculate the basic reliability indicators of the analyzed facilities, such as Mean Time To Failure – MTTF, which is the expected value of the time after which the system will fail and also failure intensity  $\lambda$ , which describes the number of failures per unit of time and is a key reliability indicator, as it informs about the frequency of failures in a given system. A Failure Rate was also calculated, which describes the probability of failure (p) in a given unit of time  $(t_p)$ , usually expressed as:

$$t_p = -\frac{\ln{(p)}}{\lambda}$$

Finally, based on the obtained results, the reliability function for the analyzed unmanned aerial vehicles was determined. Reliability function

$$R(t) = e^{-\lambda t},$$

where: R(t) is the probability that the system will operate without failure until t.

The reliability function R(t) is one of the basic characteristics used in reliability analysis. It allows you to determine the probability that the system will not fail within a certain period of time. With knowledge of the reliability function, it is possible, for example, to predict system durability, plan maintenance or preventive actions, and estimate the risk of inoperability.

#### 2.2. Analysis of identified causes of failures

First, an investigation was made into the causes of the failures that were occurring. They were classified into 6 groups, presented in Table 1.

Table 1. Failure groups of the unmanned aerial vehicle included in the study.

Type of failure	Cause
Battery failure	Overload, wear and tear, extreme temperatures
Engine / ESC failure	Overheating, mechanical wear and tear, moisture
GPS / IMU system fault	Electromagnetic interference, software errors
Communication error	Radio interference, controller failure
Frame / propellers failure	Collision, material cracks
Other failures	Software, unknown causes

The main cause of unmanned aerial vehicle (UAV) failures is battery malfunction, as batteries serve as the 'fuel' powering

these platforms. Key causes of battery failure include overload, wear, and exposure to extreme temperatures. Regarding the

database used in the study, it should be noted that it pertains exclusively to batteries from the LiPo (Lithium Polymer) group, which are currently the most commonly used power source for UAVs. LiPo battery overload is a phenomenon in which the current flowing through the circuit exceeds the rated voltage, and it may occur during the charging process.

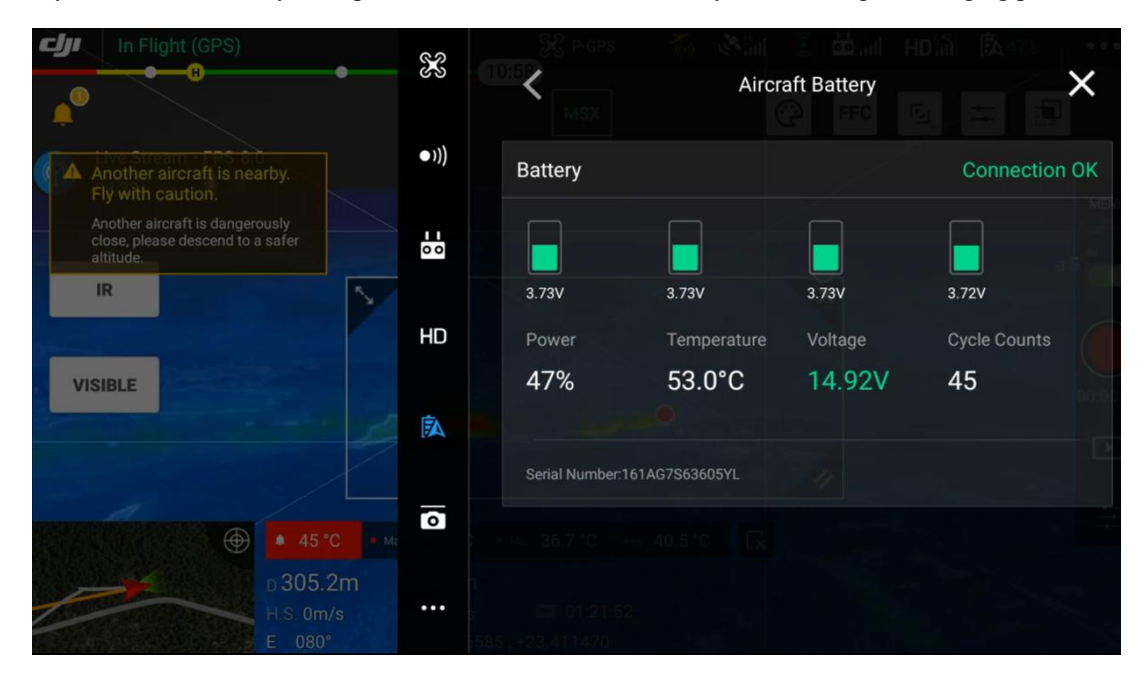


Figure 2. Battery voltage and temperature readings in the mobile application.

Although advancements in technology have led to the development of batteries that automatically adjust the charging current, traditional solutions that have been used since the beginning of unmanned aviation are still widely in use. Wear and extreme temperatures as causes of battery failure share a common factor in the context of the database: non-standard usage conditions. When it comes to saving lives, every minute counts, which is why equipment, including UAVs and their batteries, used in rescue operations is operated at full capacity – often without breaks and in diverse environmental conditions. Extremely risky operating situations are frequent, but they are the price to be paid for someone's life and health. When flying in temperature extremes for LiPo batteries – that is, beyond their operational temperature range - particular attention must be paid to continuously reading and analyzing data on the rate of voltage drop, the voltage distribution across the battery cells, and the recorded battery temperature. For the batteries selected in this study, the operating temperature range was either from – 20°C to 50°C or from −10°C to 40°C. In very low operating temperatures, batteries may discharge rapidly, leading to engine shutdowns. In high temperatures, the batteries may heat up quickly, and at around 70°C, may even explode. An example of the data recorded by the UAV during flight is presented in

Figure 2. Another type of failure occurring during UAV flights is related to motor and ESC (Electronic Speed Controller) malfunctions. The key causes of these failures include overheating, mechanical wear, and moisture. The dataset provided by the State and Volunteer Fire Service includes information recorded by UAVs equipped with brushless threephase DC motors. These motors offer high efficiency and a longer lifespan compared to brushed motors, reaching up to 90%, which results in significant energy savings and extends the operating time on a single charge [44]. Although more expensive than traditional motors, brushless motors are more cost-effective in the long term. Their design is structurally simpler than brushed motors, but they require a complex ESC control system, which manages the motor's rotational speed. Most controllers are programmable, allowing the user to set parameters directly such as motor acceleration characteristics, cutoff voltage, rotation direction, and active braking [45]. Due to the environment in which rescue operations are conducted – fire scenes and varying weather conditions - damage to both motors and ESC controllers occurs, primarily caused by exposure to fire-related conditions such as high temperatures, moisture, drizzle, as well as airborne particulates that act as heat carriers, and dust that clogs motors. An example of a message

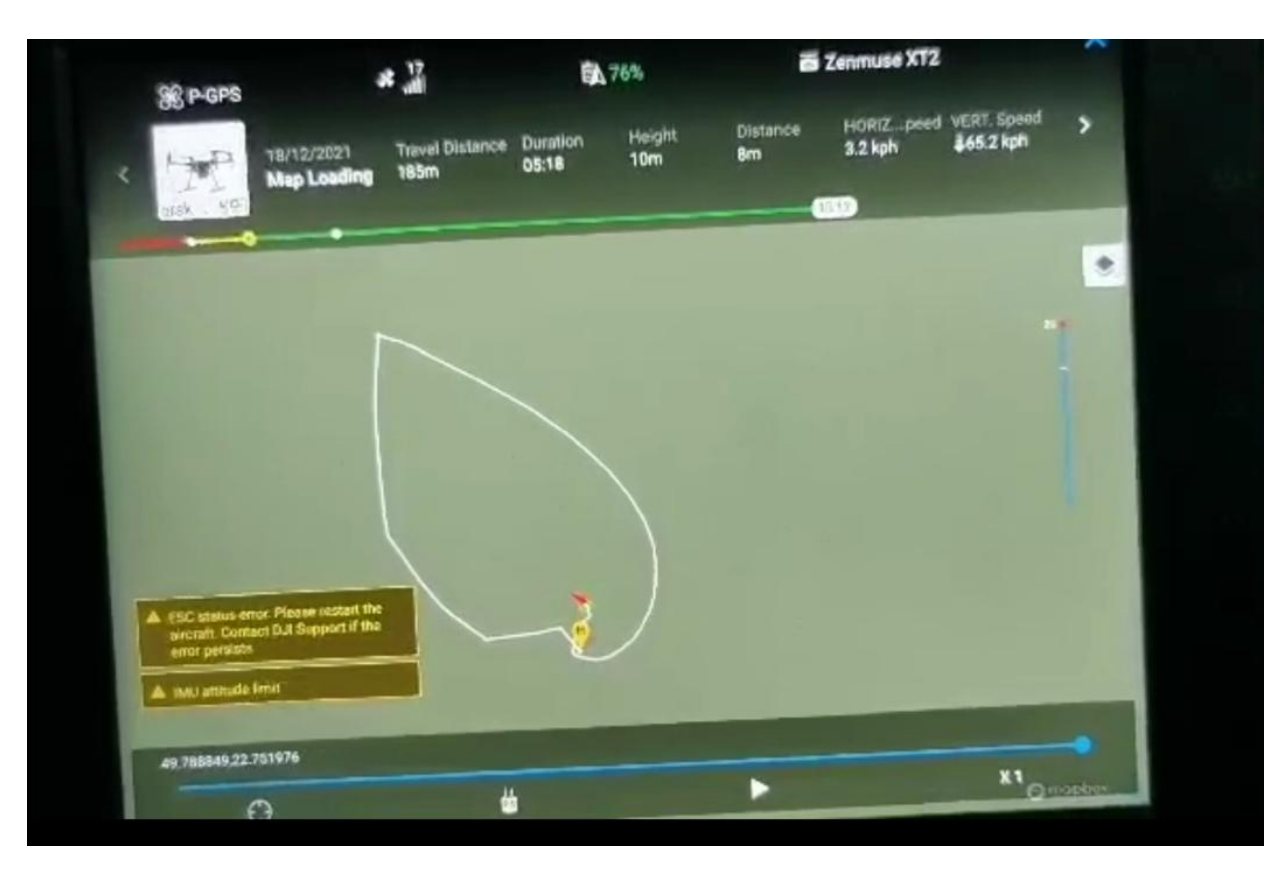


Figure 3. Message in mobile app about ESC error just before motor stop.

The next analyzed group of UAV failures includes faults in the GPS system and the IMU (Inertial Measurement Unit) caused by electromagnetic interference and software errors. In the studied UAV, the piloting modes include: Positioning (P), Sport (S), Tripod (T), and ATTI (Attitude) [46]. In the P mode, GNSS (Global Navigation Satellite System) systems, specifically the American GPS (Global Positioning System), and a downward vision system for automatic stabilization are used, allowing active braking and obstacle avoidance. In the S mode, GPS and the downward vision system enable automatic stabilization and increase the flight speed to the maximum possible value, but it cannot actively brake or avoid obstacles. In the T mode, aerial operations are performed in open space with active GPS positioning and limited flight speed. The last mode, ATTI, is manually activated by highly qualified operators performing flights in confined spaces, during which automatic positioning systems must remain inactive to give the pilot full control over UAV maneuvering. The ATTI mode is also automatically triggered by the UAV in case of GPS system failure during flights in P, S, and T modes. The automatic activation of the ATTI mode by the flying platform's software is most often caused by electromagnetic interference affecting the signal power transmitted by the controller's antenna and the signal power reaching the UAV's receiving antenna. In a rescue operation environment, key objects generating electromagnetic interference include radios used by firefighters for communication, power poles, and BTS (base transceiver station) towers used for ensuring GSM (Global System for Mobile Communication) connectivity. In addition to navigational failures related to the GPS system, there are also failures related to the inertial navigation system provided by the IMU device, which measures and reports changes in the object's motion and orientation in space using a three-axis gyroscope and a threeaxis accelerometer. Faulty IMU operations result in the UAV failing to maintain a constant altitude during an operation, a tilted horizon in the recorded images from the camera, and the UAV self-tilting. The above effects resulting from the lack of IMU calibration in the platform directly lead to hazardous situations, some of which end in equipment damage and pose safety threats to the surrounding area. An example of a presents

the IMU calibration process in the UAV is shown in Figure 4.



Figure 4. IMU calibration algorithm.

During aerial operations carried out in the context of rescue missions, failures and damage to the UAV also occur as a result of physical radio interference and/or controller malfunction. The most common source of radio interference is the fire environment. Smoke generated during a fire, as a byproduct of combustion, creates a medium that distorts the propagation of radio waves. It can also, similarly to low-level clouds, be interpreted by the optical sensor as ground, causing the platform to initiate a landing procedure, ending with the shutdown of the motors. In the event of a fire, there have also been recorded

cases of UAV controller damage caused by fine dust particles penetrating the interior of the equipment.

Due to the high-risk nature of operational flights, UAV collisions with other objects also occur, resulting in frame and propeller damage. Propellers are most commonly damaged. The operational documentation concerning flight operations also describes partial damage to the platform – failures resulting from collisions with birds, obstacles in the terrain such as trees and overhead power lines, as well as with other civilian unmanned aerial vehicles, which, by violating the ban on flying near rescue operations, caused collisions.

Flight logs maintained by Fire Protection Units, which record all aerial operations, also note other failures resulting from the malfunctioning of the mobile application installed in the controller, used to operate the UAV and the camera, display live data, and manage flights. The causes of the mobile application malfunction are often ultimately unknown, even to service technicians, as they occur cyclically, regardless of the location, time, or environment of the aerial operation, and the application itself does not log these errors. Therefore, some of these failures form a group of failures of unknown origin.

The time-to-failure distribution for the above-mentioned groups is shown in Figure 5.

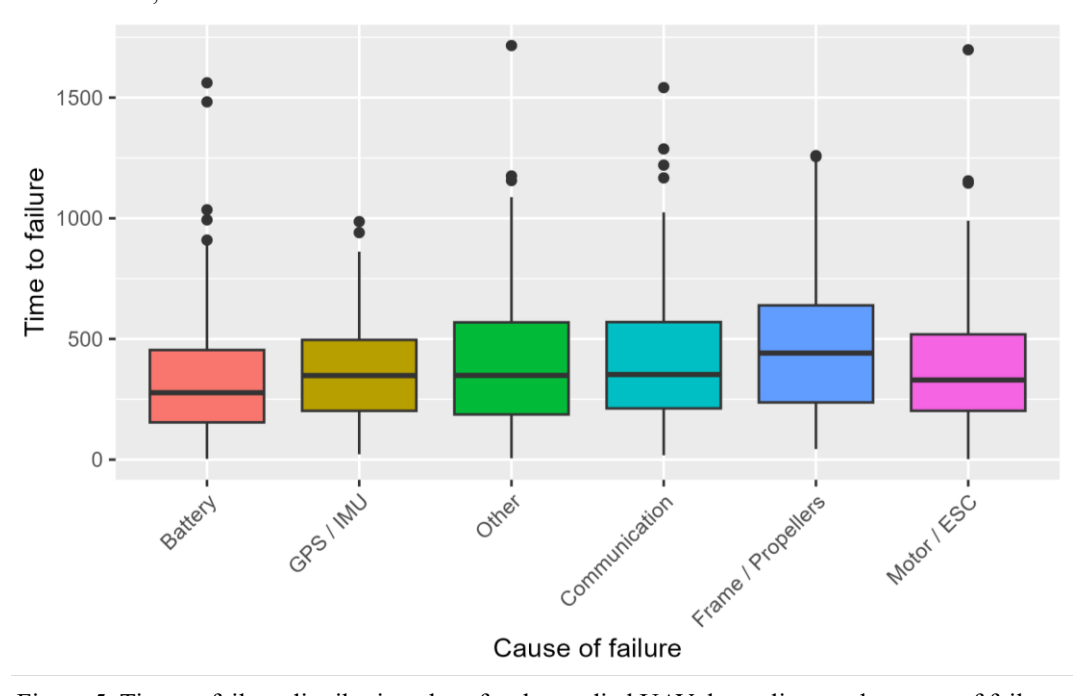


Figure 5. Time to failure distribution chart for the studied UAV depending on the cause of failure.

Next, the assumption of normality was verified, which allows for the application of tests dedicated to this type of distribution or the exclusion of such a possibility. Normality tests were performed using the Kolmogorov-Smirnov test, and the results are presented in Table 2.

Table 2. Kolmogorov-Smirnov test results for time-to-failure in individual failure cause groups.

Cause	Value of test statistic D	p-value
Transport	0.11904	0.1321
Battery	0.10189	0.00295
Frame / Propellers	0.1044	0.2981
GPS / IMU	0.063074	0.5517
Motor / ESC	0.10665	0.009758
Other	0.11298	0.1035

For most distributions, the assumption of normality was not confirmed. Therefore, to verify whether the cause of the malfunction significantly affects the time to failure, the non-parametric Kruskal-Wallis test was used. The test statistic was chi-squared = 26.545 and p-value =  $6.993*10^{-5}$ , hence there is no basis to reject the null hypothesis, and in further analysis, it

is assumed that at least two distributions differ significantly from each other. To determine which distributions differ significantly, a series of Wilcoxon tests was performed between all possible pairs of groups, using the *p*-value correction method to account for multiple comparisons (Table 3).

Table 3. Wilcoxon test results for individual group pairs.

	Battery	GPS / IMU	Other	Communication	Frame / Propellers
GPS / IMU	0.024				
Other	0.025	0.865			
Communication	0.053	0.926	0.926		
Frame /Propellers	$7.8 * 10^{-5}$	0.026	0.105	0.102	
Motor / ESC	0.024	0.941	0.853	0.913	0.024

A significant difference in time to failure was observed for most comparisons involving the failure cause classified as Battery. Differences were noted for the following pairings: GPS / IMU (p = 0.024), Other (p = 0.025), Frame / Propellers (p = 0.000078), and Motor / ESC (p = 0.024). Additionally, significant differences were found between Frame / Propellers and GPS / IMU (p = 0.026), as well as between Motor / ESC and Frame / Propellers (p = 0.024). This indicates that these types of malfunctions significantly differ in terms of time to failure. In the remaining groups, the cause of failure does not significantly affect UAV operating time.

The relationship between battery failures and other failure types may result from the platform and its subsystems being directly dependent on the power source. Moreover, the battery is the only platform component whose lifespan and failure rate are influenced not only by flight operation time but also by maintenance practices – such as charging method (charging voltage), discharging, storage procedures, and storage temperature.

To further investigate and compare the impact of individual factors on time to failure, the Kaplan-Meier survival analysis method was applied. For each analyzed group of failure-causing factors, a survival function was estimated, and the course of this function was visually compared across the groups. Survival curves enable quick identification of factors associated with the occurrence of failures, as shown in Figure 6.

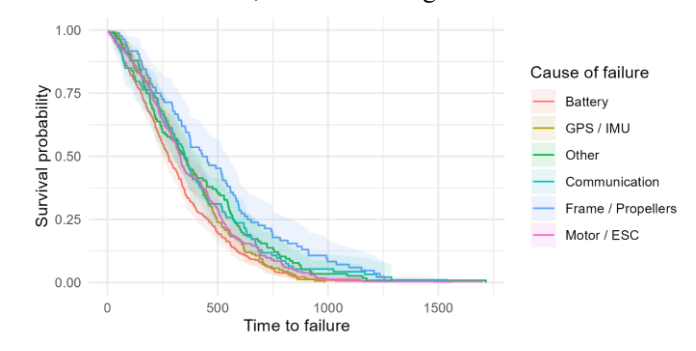


Figure 6. Kaplan-Meier survival analyses for each of the analyzed groups of failure-causing factors.

The group defined by failure causes related to the Battery shows the greatest deviation, although no drastic differences are visible on the graph. Nevertheless, in the Battery group, failures occur significantly faster than in the others (a higher number of failures, shorter survival time), which is also confirmed by the log-rank test conducted to provide a detailed comparison of the

survival curves (Table 4).

Table 4. Log-rank test results.

Failure Cause	N	Observed	Expected	$(\boldsymbol{O}-\boldsymbol{E})^2/\boldsymbol{E}$	$(\boldsymbol{O}-\boldsymbol{E})^2/V$
Battery	314	314	254	14.24283	19.2935
GPS / IMU	159	159	151	0.41932	0.4984
Other	116	116	133	2.20967	2.5788
Transport	93	93	104	1.17026	1.3152
Frame / Propellers	84	84	123	12.10361	14.1008
Motor / ESC	234	234	235	0.00828	0.0109

Where  $(O - E)^2/E$  is an indicator of how much the actual number deviates from the expected – the larger the value, the greater the contribution to the test statistic while  $(O - E)^2/V$  takes into account the variance in addition.

The test statistic Q=31.1, and the value  $p=9*10^{-6}$ , so the result is statistically significant. The failure rate for the Battery turned out to be higher than expected (314 observed vs 254 expected), while a slight difference in favor of the observed value was noted for GPS / IMU. In the case of Communication, Frame / Propellers, and Other, there were fewer failures than

expected, whereas for Motor / ESC the values are nearly consistent.

# 2.3. Analysis of Identified Failures in the Context of Weather Conditions

Subsequently, a study was conducted on failures depending on the weather conditions, as presented in Table 5 and the distribution of time to failure for each group, as shown in Figure 7.

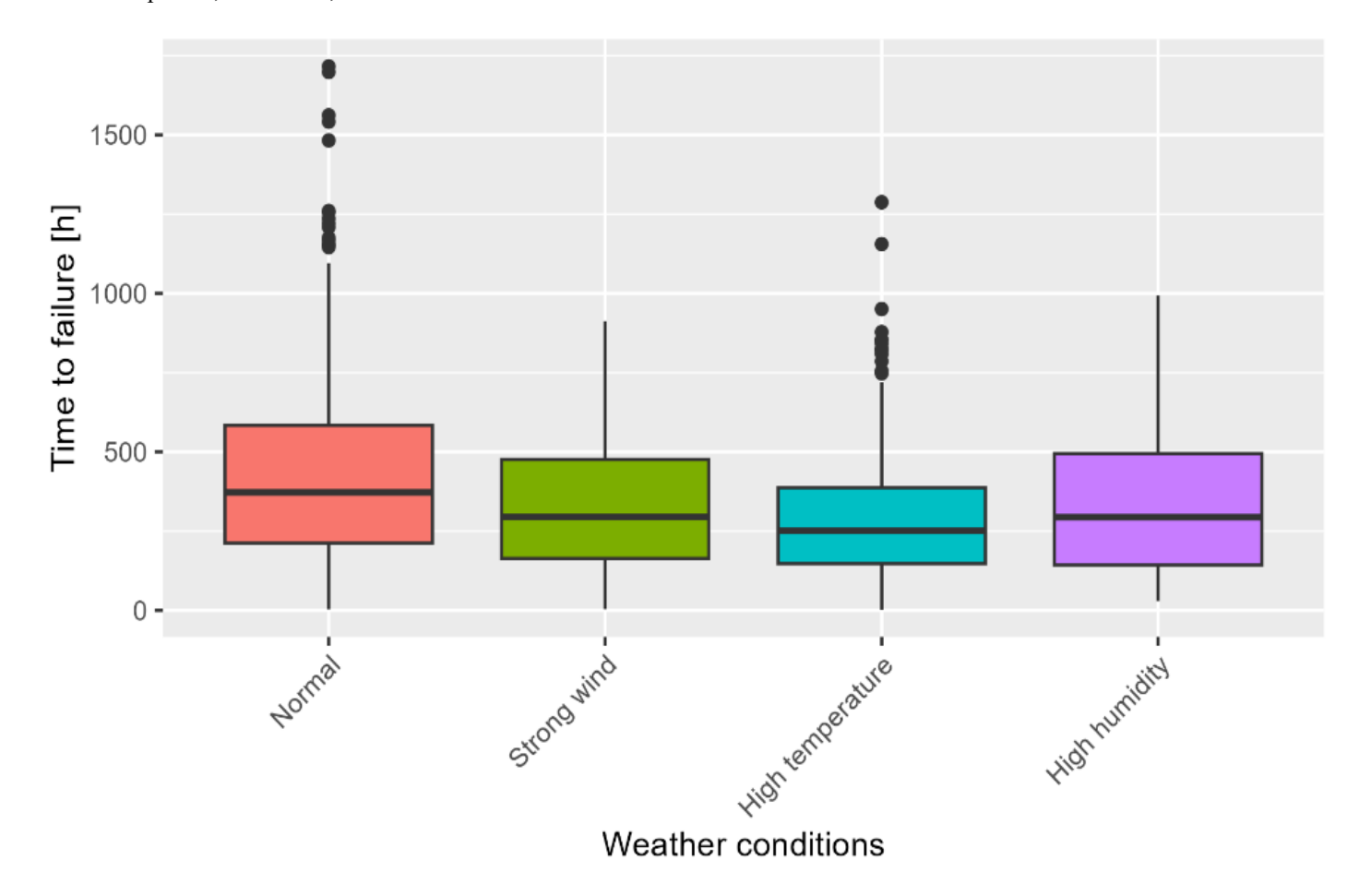


Figure 7. The distribution of time to failure for the studied aircraft based on weather conditions.

Table 5. Failure groups of the unmanned aerial vehicle included in the study.

Weather factor	Characteristic
Normal	Wind speeds < 8 m/s; ambient temperature of 15°C, no precipitation
Strong wind	Wind speeds of around 15 m/s during flight and about 12 m/s during takeoff and landing
High temperature	Extreme operating conditions for the platform and battery: -20°C and 50°C
High humidity	High humidity for the platform used in the study is indicated by the presence of water particles
	on the housing and propellers after landing

The characteristic values of selected weather factors used in the study are based on the values specified by the manufacturer in the user manual of the UAV used for data collection. According to the manufacturer's data, normal weather conditions can be considered as wind speeds up to approximately 8 m/s, ambient temperature of 15°C, and no precipitation. Strong winds for the selected UAV model refer to wind speeds of around 15 m/s during flight and about 12 m/s during takeoff and landing. Values indicating high temperatures

are extreme operating conditions for the platform and battery: – 20°C and 50°C. High humidity for the platform used in the study is indicated by the presence of water particles on the housing and propellers after landing, which are equivalent to water droplets generated by a 12.5 dm³/min water spray impacting the platform.

Similarly, an analysis of the normality of the distributions separated by the weather factor was conducted using the Kolmogorov-Smirnov test (Table 6).

Table 6. Kolmogorov-Smirnov test results for time-to-failure in individual weather factor groups.

Weather factor	Value of test statistic D	p-value
Normal	0.082703	0.00146
Strong wind	0.08996	0.1034
High temperature	0.12677	0.003443
High humidity	0.099264	0.3105

At the significance level  $\alpha = 0.05$ , normality was confirmed only for the factors Strong Wind and High Humidity. The lack of normality in the remaining groups led to the reexamination of differences using the Kruskal-Wallis test. The Table 7. Wilcoxon test results for individual group pairs.

test statistic KW = 43.097, and the p-value =  $2.347*10^{-9}$ . To identify which pairs of groups differ significantly, the Wilcoxon test with p-value correction was used, and its results are presented in Table 7.

 Normal
 Strong wind
 High temperature

 Strong wind
 0.00024 0.12285 

 High temperature
  $3.4*10^{-8}$  0.12285 

 High humidity
 0.00411 0.82449 0.34037

The time to failure was significantly shorter in all adverse weather conditions compared to normal conditions, while no significant differences were observed between the various adverse conditions (wind, temperature, humidity).

To visualize and compare the influence of each weather factor on the time to failure, a Kaplan-Meier survival analysis was conducted again, and the survival function was plotted, as shown in Figure 8 with the results presented in table 8.

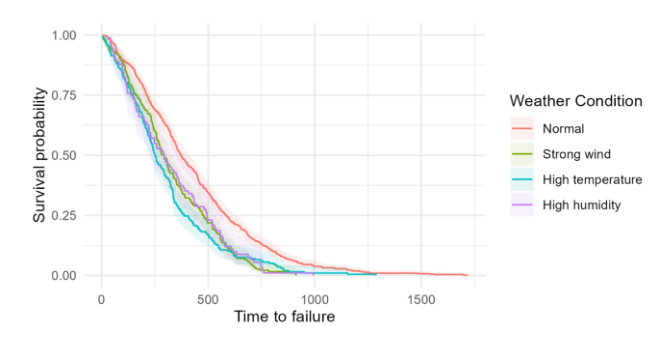


Figure 8. Kaplan-Meier survival analyses for each of the analyzed groups of weather factors.

Table 8. Log-rank test results in each group of causes.

Failure Cause	N	Observed	Expected	(O-E)^2/E	(O-E)^2/V
Normal	528	528	633	17.49	49.41
Strong wind	183	183	147	9.07	10.81
High temperature	198	198	146	18.34	21.67
High humidity	91	91	74	3.90	4.24

The log-rank test showed statistically significant differences in the time to failure between weather conditions ( $\chi^2 = 50.5$ , p =  $6*10^{-8}$ ). Fewer failures than expected, and thus better survival, were recorded under normal conditions, while in the case of strong winds, high temperature, and high humidity, there were more failures than expected, indicating worse survival. The largest difference from expectations – the greatest deviations from the 'norm' – concerned high temperatures (18.34) and normal conditions (17.49).

#### 3. Analysis of non-failure operating time

Next, the non-failure operating time was analyzed by first selecting an appropriate probabilistic model to describe this distribution. In literature and engineering practice, one of the most commonly used distributions is the Weibull distribution, often applied in the analysis of durability, reliability, and failure risk assessment of devices, although other distributions are also used [3]. The Weibull distribution is highly flexible – depending

on the shape parameter (k), it allows modeling different failure mechanisms:

k < 1 – random failures, e.g., manufacturing defects,

k = 1 – constant failure risk (corresponding to an exponential distribution),

k > 1 – wear and aging of devices (failure risk increases with time).

For this reason, the Weibull distribution is a universal initial model, allowing the examination of both random failure characteristics and their dependence on operating time. However, the consistency with other distributions, commonly used in reliability analysis, was also checked. To determine which distribution best describes the non-failure operating time of drones, a comparison of four models was made: Weibull, exponential (exp), log-normal (lnorm), and gamma (Table 9). The goodness-of-fit evaluation was performed based on fit statistics and information criteria (AIC and BIC) (Goodness-of-fit criteria).

Table 9. Compliance statistics and information criteria for proposed distributions.

Model	weibull	exp	lnorm	gamma
Goodness-of-fit statistics		·		
Kolmogorov-Smirnov statistic	0.019	0.141	0.084	0.035
Cramer-von Mises statistic	0.060	6.940	2.672	0.337
Anderson-Darling statistic	0.409	38.002	16.146	2.037
Goodness-of-fit criteria				
Akaike's Information Criterion	13672.65	13862.81	13890.21	13689.28
Bayesian Information Criterion	13682.47	13867.72	13900.03	13699.10

The Kolmogorov-Smirnov, Cramér-von Mises, and Anderson-Darling statistics allow for assessing how well a theoretical distribution fits the empirical data. The smaller the values of these statistics, the better the fit. Analyzing the results in

, it can be concluded that the exponential distribution poorly fits the data – especially the sensitive tests (Cramér-von Mises and Anderson-Darling), which show very large values. The results for the Weibull and Gamma distributions are similar (and the best). Akaike's Information Criterion (AIC) and the Bayesian Information Criterion (BIC) are used to assess the

quality and compare competing models. Both criteria are based on the principle of balancing the goodness-of-fit of the model to the empirical data with its structural complexity. The lowest values for AIC and BIC are associated with the Weibull distribution (slightly better than Gamma). Ultimately, considering both the fit statistics and the information criteria,

the most adequate model can be considered to be the Weibull distribution. The fit of this distribution to the empirical data is presented the Figure 9.:

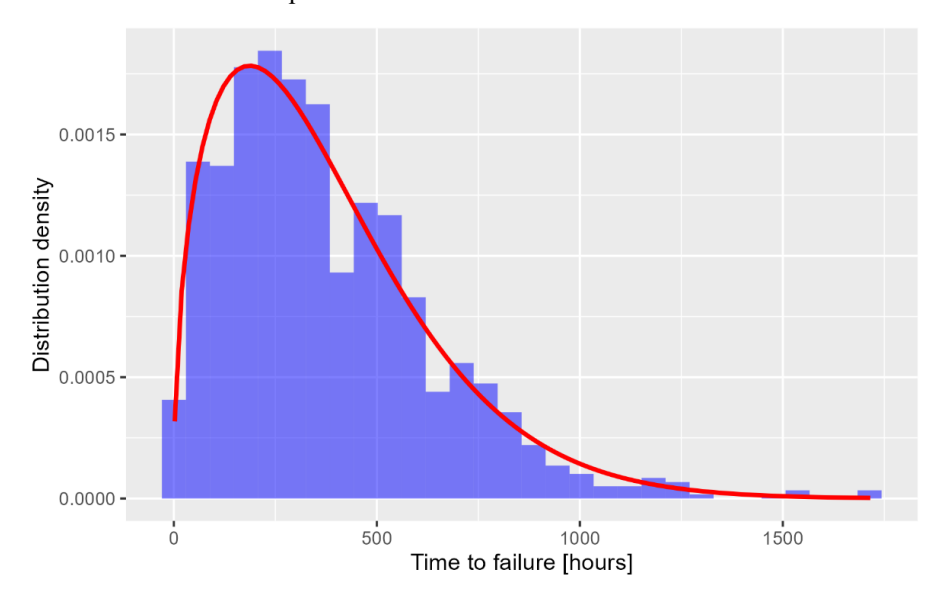


Figure 9. Empirical data and fitted Weibull distribution.

The parameters of the fitted distribution are shape k = 1.455 and scale  $\lambda = 414.888$ .

In the next step, failure behavior modeling was performed using Monte Carlo simulation to estimate the predicted mean time to failure of the studied type of UAV, based on the previously fitted Weibull distribution. Monte Carlo simulation allows for incorporating randomness and uncertainty in

forecasting failure time. This enables a better understanding of risk and a more realistic approach to service planning, inspections, and equipment replacement.

A total of  $10^4$  independent Monte Carlo simulation replications were performed. In each iteration, a random sample of size  $n=10^3$  observations was generated from the Weibull distribution. These realizations modeled the failure times of UAVs. The simulation results are presented the Figure 10.

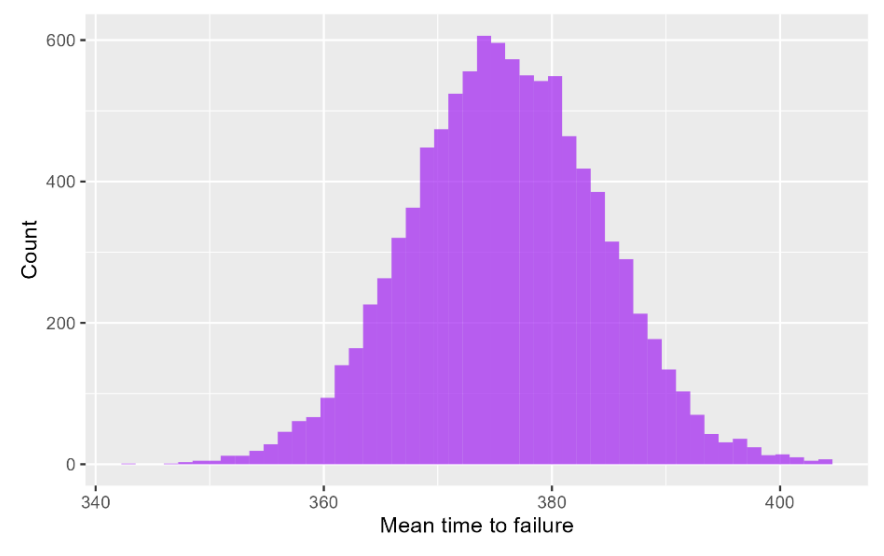


Figure 10. Mean time to failure based on Monte Carlo simulation

Based on the conducted simulations, basic reliability indicators for the studied objects were calculated. The MTTF (Mean Time To Failure) was 376.3 hours. This is the average time after which the UAV will fail. Therefore, the UAV will

operate without failure for about 376.3 hours, and after this time, a failure occurs on average. The MTBF (Mean Time Between Failures) also equaled 376.3 hours, as the average time between subsequent failures in a system consisting of only one

component is equal to the MTTF. This is because after each failure, the system is restored to its initial state and operates again until the next failure. The failure intensity ( $\lambda$ ) represents the average number of failures occurring per unit of time – the lower the value of  $\lambda$ , the more reliable the system. In the analyzed case  $\lambda = 0.00266$ , thus there is approximately a 0.00266 chance of failure occurring per time unit.

Next, the reliability function was determined, which describes the probability that the examined UAV will operate without failure for a specified time t,

$$R(t) = e^{-\lambda t}$$

where R(t) is the probability that the system will function without failure until time t, and  $\lambda$  is the previously determined failure intensity (in this case, 0.00266 per hour).

The reliability function R(t) is one of the fundamental characteristics used in reliability analysis. It allows you to

determine the probability that the system will not fail within a certain period of time. A characteristic feature of this function is that its curve is decreasing - as time t increases, the probability of failure-free operation of the system gradually decreases. At the beginning of the operation R(0) = 1, which means that right after the system is started, it will certainly operate without failure. As time passes, the value of the reliability function approaches zero, reflecting the increasing risk of failure. With knowledge of the reliability function, it is possible, for example, to predict system durability, plan maintenance or preventive actions, and estimate the risk of inoperability. The function graphs shown in Figure 11 represent the probabilities of failure-free operation in the free time range. Based on it, one can determine how long the system maintains a high probability of reliability and at what point the risk of failure becomes significant.

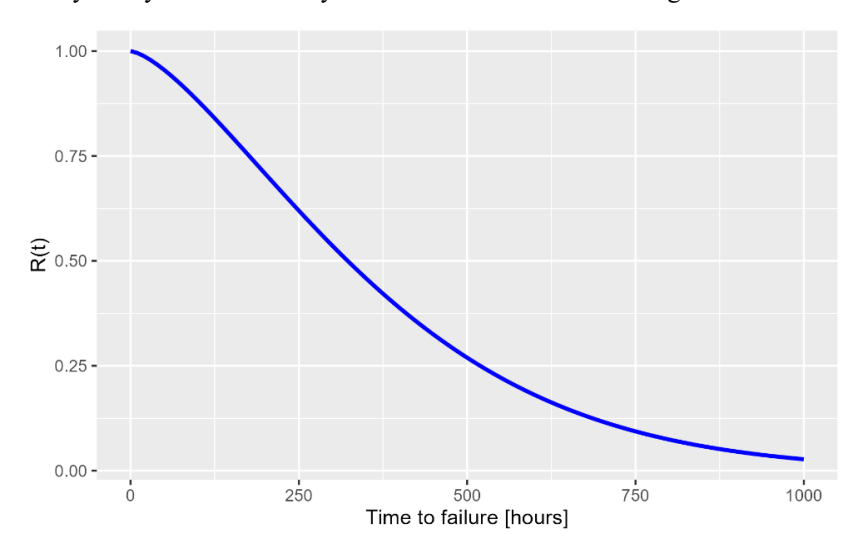


Figure 11. Reliability function of the tested UAV.

The Failure Rate indicator was computed – the time to reach a certain reliability level, which informs how long the system operates before the probability of failure exceeds a specified threshold. In this case, a 50% probability was assumed, and calculations were made according to the formula:

$$R(t=0.5) = \frac{-\log(0.5)}{\lambda}$$

The value R(t = 0.5) was 260.8364, meaning that on average, the UAV will operate for over 260 hours before the probability of failure exceeds 50%.

#### 4. Discussion of the results

The results of the statistical analysis conducted in this study showed that in most comparisons between pairs of failure causes, there are significant differences in the time to failure. These differences were most often observed in failures related to the battery, and the results suggest that the way and mechanism of these particular failures could significantly influence the UAV's operational time until failure. In contrast, no statistically significant differences in time to failure were observed in other comparisons, including those related to GPS/IMU, Communication, or the 'Other' category. This may suggest that, regardless of the type of failure in these groups, the UAV's operating time until failure is similar. These results may imply that the cause of failure in these cases is less related to the operational time and more associated with random factors or external conditions.

An analysis of the impact of general weather conditions on time to failure was also conducted. The variable describing weather conditions was categorical and included four main groups: normal weather conditions, strong wind, high temperature and high humidity. It should be emphasized that during this stage of the research, the weather data were simplified and qualitative – they were collected in a general manner without precise numerical values, such as specific wind speeds, temperature levels, or humidity levels.

The statistical tests performed showed that the time to failure under conditions considered unfavorable (strong wind, high temperature, high humidity) was significantly shorter compared to normal conditions. At the same time, no statistically significant differences in time to failure were found between the different unfavorable weather conditions. This result suggests that regardless of the type of adverse weather factor, each of them similarly contributed to an increase in the system's failure rate.

Based on the simulations conducted, it can be concluded that the studied UAV demonstrates relatively high reliability during the initial period of operation. The MTTF and MTBF values of approximately 376.3 hours indicate that the average time of failure-free operation of the system is relatively long. This is also confirmed by the low failure rate intensity value of  $\lambda = 0.00266$ , which means that the probability of a failure occurring within a given time unit is small. Such parameters are particularly important in systems where reliability plays a key role, such as in the case of the studied rescue services. The computed values provide valuable information for planning maintenance and managing the system's lifecycle, as well as in the context of the readiness and reliability of the structures of the State and Volunteer Fire Departments.

The analysis of the reliability function R(t) provides additional insight into the dynamics of the decline in the probability of failure-free operation of the UAV over time. It indicates that the system maintains high reliability during the first few hundred hours of operation, while a significant decrease in reliability occurs only after about 260 hours, when the probability of failure exceeds 50%. In practice, this means that service or preventive actions should be planned based on this time frame to minimize the risk of unexpected downtime or system failures. Therefore, the results of the simulations not

only characterize the reliability of the studied object but also serve as a practical tool to support the management of its operation.

#### 5. Conclusion

The conducted research allowed for the preliminary determination of the relationship between the type of failure and the time to its occurrence in the unmanned aerial vehicle, as well as the weather conditions, which were considered at a high level of generalization. It was shown that for some types of failures, such as battery or frame/propeller damage, the time to failure differs significantly from other types of failures. On the other hand, for other failures, such as GPS/IMU, communication issues, or elements classified as 'Other', the time to failure remains at a similar level. Additionally, adverse weather conditions, regardless of their type, had a significant impact on shortening the failure-free operating time. However, considering the limitations arising from the qualitative nature of the weather data, the obtained results should be regarded as preliminary and exploratory. Therefore, future research will expand data collection to include detailed and quantitative meteorological information. In particular, it is planned to collect precise measurements of air temperature, wind speed and direction, relative humidity, and other relevant environmental parameters. This will allow for more advanced statistical analyses and modeling of the relationship between weather conditions and system reliability. Moreover, it will be possible to identify critical thresholds for individual atmospheric parameters, above which the risk of failure increases significantly.

Nonetheless, the obtained results, in combination with the calculated system reliability indicators, provide valuable information for planning technical maintenance and managing the operational readiness of UAVs used in rescue services.

It is also worth mentioning that in order to minimize the risk of aircraft failures in emergency services, it is crucial to implement comprehensive maintenance procedures, systematic staff training and constant monitoring of flight parameters. Maintenance should go beyond standard periodic inspections and include extended non-destructive testing of key structural elements, especially in units operated in difficult conditions. It is recommended to keep digital records of faults, analyze failure

trends and apply preventive maintenance - replacing elements before reaching the wear limit. It is equally important to provide UAV pilots with access to manufacturer training and regular training courses, which increases the effectiveness and quality of technical service.

UAV pilots should regularly participate in simulator training, including in the field of response to failures and crisis management. Joint exercises of pilots and rescuers increase the effectiveness of rescue operations in the field. At the same time, flight parameter monitoring systems should be implemented, which allow for ongoing analysis of the technical condition of the UAV and detect potential faults before they lead to failure. These activities should be complemented by a safety culture based on open incident reporting and a thorough analysis of weather and operational conditions before each mission. Integrating these elements into the daily operational practice of

emergency services significantly increases the level of flight safety and reduces the risk of serious failures.

It should be emphasized that the presented results are just the starting point for further, more detailed studies. In the future, it is recommended to expand the analyses with a larger number of variables describing both the technical state of the system and environmental conditions in the form of precise numerical data rather than categories. A significant direction for the development of research is also the detailed analysis of individual types of failures, considering their specificity and potential causes. Additionally, the application of more advanced analytical methods, including machine learning models, could enable the identification of hidden dependencies and the development of effective failure prediction algorithms, supporting preventive maintenance actions and increasing the reliability of UAV systems.

#### References

- Al-Haddad, L. A., Giernacki, W., Shandookh, A. A., Jaber, A. A., Puchalski, R. Vibration Signal Processing for Multirotor UAVs Fault Diagnosis: Filtering or Multiresolution Analysis?. Eksploatacja i Niezawodność – Maintenance and Reliability 2024; 26(1), https://doi.org/10.17531/ein/176318.
- Szczupak, P., Kossowski, T., Szostek, K., Szczupak, M. Tests of pulse interference from lightning discharges occurring in unmanned aerial vehicle housings made of carbon fibers. Eksploatacja i Niezawodność – Maintenance and Reliability 2025; 27(1), https://doi.org/10.17531/ein/193984.
- 3. Kozłowski, E., Borucka, A., Oleszczuk, P., Leszczyński, N. Evaluation of readiness of the technical system using the semi-Markov model with selected sojourn time distributions. Eksploatacja i Niezawodność Maintenance and Reliability 2024; 26(4), https://doi.org/10.17531/ein/191545.
- 4. Jaroń A, Borucka A, Deliś P, Sekrecka A. An Assessment of the Possibility of Using Unmanned Aerial Vehicles to Identify and Map Air Pollution from Infrastructure Emissions. Energies 2024; 17(3): 577, https://doi.org/10.3390/en17030577.
- 5. Mohsan, S. A. H., Othman, N. Q. H., Li, Y., Alsharif, M. H., & Khan, M. A. Unmanned aerial vehicles (UAVs): Practical aspects, applications, open challenges, security issues, and future trends. Intelligent service robotics 2023; 16(1): 109-137, https://doi.org/10.1007/s11370-022-00452-4.
- 6. Manning, S. D., Rash, C. E., Leduc, P. A., Noback, R. K., & McKeon, J. The role of human causal factors in US Army unmanned aerial vehicle accidents. US Army 2004; 20040409, 013, https://doi.org/10.21236/ADA421592.
- 7. Oncu, M., & Yildiz, S. An analysis of human causal factors in unmanned aerial vehicle (uav) accidents. Doctoral dissertation, Monterey, California: Naval Postgraduate School: 2014, https://doi.org/10.21236/ADA620843.
- 8. Ghasri, M., & Maghrebi, M. Factors affecting unmanned aerial vehicles' safety: A post-occurrence exploratory data analysis of drones' accidents and incidents in Australia. Safety science 2021; 139: 105273, https://doi.org/10.1016/j.ssci.2021.105273.
- 9. Shafiee, M., Zhou, Z., Mei, L., Dinmohammadi, F., Karama, J., & Flynn, D. Unmanned Aerial Drones for Inspection of Offshore Wind Turbines: A Mission-Critical Failure Analysis. Robotics 2021; 10(1): 26, https://doi.org/10.3390/robotics10010026.
- 10. Grindley, B., Phillips, K., Parnell, K. J., Cherrett, T., Scanlan, J., & Plant, K. L. Over a decade of UAV incidents: A human factors analysis of causal factors. Applied Ergonomics 2024; 121: 104355, https://doi.org/10.1016/j.apergo.2024.104355.
- 11. Duffy, J. P., Cunliffe, A. M., DeBell, L., Sandbrook, C., Wich, S. A., Shutler, J. D., ... & Anderson, K. Location, location, location: considerations when using lightweight drones in challenging environments. Remote Sensing in Ecology and Conservation 2018; 4(1): 7-

- 19, https://doi.org/10.1002/rse2.58.
- 12. Haugse, S. Investigation of UAV related incidents and accidents. Master's thesis, UiT The Arctic University of Norway: 2022.
- 13. Cabahug, J., & Eslamiat, H. Failure Detection in Quadcopter UAVs Using K-Means Clustering 2022; 22(16): 6037, https://doi.org/10.3390/s22166037.
- 14. Tian, H., & Wang, F. Research on Fault-Tolerant Control Technology for Large UAV with Full Engine Failure. Proceedings of 4th 2024 International Conference on Autonomous Unmanned Systems (4th ICAUS 2024): Volume IV. Vol. 1377. Springer Nature: 2025, http://dx.doi.org/10.1007/978-981-96-3568-9\_25.
- 15. Wanner, D., Hashim, H. A., Srivastava, S., & Steinhauer, A. UAV avionics safety, certification, accidents, redundancy, integrity, and reliability: a comprehensive review and future trends. Drone Systems and Applications 2024; 12: 1-23, https://doi.org/10.1139/dsa-2023-0091.
- 16. Xing, L., & Johnson, B. W. Reliability theory and practice for unmanned aerial vehicles. IEEE Internet of Things Journal 2022; 10(4): 3548-3566, https://doi.org/10.1109/JIOT.2022.3218491.
- 17. Shafiee, M., Zhou, Z., Mei, L., Dinmohammadi, F., Karama, J., & Flynn, D. (2021). Unmanned Aerial Drones for Inspection of Offshore Wind Turbines: A Mission-Critical Failure Analysis. Robotics 2021; 10(1): 26, https://doi.org/10.3390/robotics10010026.
- 18. Hedayati, M., Barzegar, A., & Rahimi, A. Fault Diagnosis and Prognosis of Satellites and Unmanned Aerial Vehicles: A Review. Applied Sciences 2024; 14(20): 9487, https://doi.org/10.3390/app14209487.
- 19. Wang, D., Li, S., Xiao, G., Liu, Y., & Sui, Y. An exploratory study of autopilot software bugs in unmanned aerial vehicles. In Proceedings of the 29th ACM joint meeting on European software engineering conference and symposium on the foundations of software engineering: 2021: 20-31, https://doi.org/10.1145/3468264.3468559.
- 20. Di Sorbo, A., Zampetti, F., Visaggio, A., Di Penta, M., & Panichella, S. Automated identification and qualitative characterization of safety concerns reported in uav software platforms. ACM Transactions on Software Engineering and Methodology 2023; 32(3): 1-37, https://dl.acm.org/doi/10.1145/3564821.
- 21. Sziroczak, D., Rohacs, D., & Rohacs, J. Review of using small UAV based meteorological measurements for road weather management. Progress in Aerospace Sciences 2022; 134: 100859, https://doi.org/10.1016/j.paerosci.2022.100859.
- 22. Averyanova Y., Znakovskaja E. Weather Hazards Analysis for small UASs Durability Enhancement, 2021 IEEE 6th International Conference on Actual Problems of Unmanned Aerial Vehicles Development (APUAVD), Kyiv, Ukraine: 2021: 41-44, doi: 10.1109/APUAVD53804.2021.9615440.
- 23. Mohsan, S. A. H., Khan, M. A., Noor, F., Ullah, I., & Alsharif, M. H. Towards the Unmanned Aerial Vehicles (UAVs): A Comprehensive Review. Drones 2022; 6(6): 147, https://doi.org/10.3390/drones6060147.
- 24. López, B., Muñoz, J., Quevedo, F., Monje, C. A., Garrido, S., & Moreno, L. E. Path Planning and Collision Risk Management Strategy for Multi-UAV Systems in 3D Environments. Sensor 2021; 21(13): 4414, https://doi.org/10.3390/s21134414.
- 25. Li, Y., Ding, Q., Li, K., Valtchev, S., Li, S., & Yin, L. A survey of electromagnetic influence on UAVs from an EHV power converter stations and possible countermeasures. Electronics 2021; 10(6): 701, https://doi.org/10.3390/electronics10060701.
- 26. Li, Y., Hu, M., Liang, M., Chen, S., Zhou, T., & Yuan, X. Study on the Effects of Ultra-Wideband Electromagnetic Pulses on Unmanned Aerial Vehicles. IEEE Transactions on Electromagnetic Compatibility 2024, http://dx.doi.org/10.1109/TEMC.2024.3386551.
- 27. Perz, R. Wielowymiarowe zagrożenia związane z bezzałogowymi systemami powietrznymi: badanie biomechanicznych, technicznych, operacyjnych i prawnych rozwiązań zapewniających bezpieczeństwo i ochronę. Archiwum Transportu 2024; 69(1): 91-111,
- 28. Nisser, T., & Westin, C. Human factors challenges in unmanned aerial vehicles (uavs): A literature review. School of Aviation of the Lund University, Ljungbyhed: 2006.
- 29. Kasprzyk, P. J., & Konert, A. Reporting and investigation of Unmanned Aircraft Systems (UAS) accidents and serious incidents. Regulatory perspective. Journal of Intelligent & Robotic Systems 2021;103(1): 3, https://doi.org/10.1007/s10846-021-01447-6.
- 30. Wanner, D., Hashim, H. A., Srivastava, S., & Steinhauer, A. UAV avionics safety, certification, accidents, redundancy, integrity, and reliability: a comprehensive review and future trends. Drone Systems and Applications 2024; 12: 1-23, https://doi.org/10.1139/dsa-2023-0091.
- 31. Clothier, R. A., Williams, B. P., & Hayhurst, K. J. Modelling the risks remotely piloted aircraft pose to people on the ground. Safety science

- 2018; 101: 33-47, https://doi.org/10.1016/j.ssci.2017.08.008.
- 32. Ghazali, M. H. M., & Rahiman, W. Vibration-based fault detection in drone using artificial intelligence. IEEE Sensors Journal 2022; 22(9): 8439-8448, https://doi.org/10.1109/JSEN.2022.3163401.
- 33. Iannace, G., Ciaburro, G., & Trematerra, A. Fault diagnosis for UAV blades using artificial neural network. Robotics 2019; 8(3): 59, https://doi.org/10.3390/robotics8030059.
- 34. Hentati, A. I., Fourati, L. C., Elgharbi, E., & Tayeb, S. Simulation tools, environments and frameworks for UAVs and multi-UAV-based systems performance analysis (version 2.0). International Journal of Modelling and Simulation 2023; 43(4): 474-490, http://dx.doi.org/10.1080/02286203.2022.2092257.
- 35. Mishra, A., Pal, S., Malhi, G. S., & Singh, P. R. A. B. H. A. T. Structural analysis of UAV airframe by using FEM techniques: A review. International Journal of Advanced Science and Technology 2020; 29: 195-204.
- 36. Salazar, J. C., Sanjuan Gómez, A., Nejjari Akhi-Elarab, F., & Sarrate Estruch, R. Health-aware and fault-tolerant control of an octorotor UAV system based on actuator reliability. International journal of applied mathematics and computer science 2020; 30(1): 47-59, http://dx.doi.org/https://doi.org/10.34768/amcs-2020-0004.
- 37. Salazar, S., Flores, J., González-Hernández, I., Rosales-Luengas, Y., & Lozano, R. Robust Control for a Slung-Mass Quadcopter Under Abrupt Velocity Changes. Applied Sciences 2024; 14(24): 11592, https://doi.org/10.3390/app142411592.
- 38. Kruskal, W. H., & Wallis, W. A. Use of ranks in One-Criterion Variance Analysis. Journal of the American statistical Association 1952; 47(260): 583-621, https://doi.org/10.2307/2280779.
- 39. Kolmogorov A. Sulla determinazione empirica di una legge di distribuzione. Giorn Dell'inst Ital Degli Att 1993; 4: 89-91.
- 40. Smirnov N. Table for estimating the goodness of fit of empirical distributions. Annals of Mathematical Statistics 1948; 19 (2): 279–281, https://doi.org/10.1214/aoms/1177730256.
- 41. Zakaria, S., Mahadi, M. R., Abdullah, A. F., & Abdan, K. (2019). Aerial platform reliability for flood monitoring under various weather conditions: A review 2019; 295-314, http://dx.doi.org/10.5194/isprs-archives-XLII-3-W4-591-2018.
- 42. Gao, M., Hugenholtz, C. H., Fox, T. A., Kucharczyk, M., Barchyn, T. E., & Nesbit, P. R. Weather constraints on global drone flyability. Scientific reports 2021; 11(1): 12092, http://dx.doi.org/10.5194/isprs-archives-XLII-3-W4-591-2018.
- 43. Omolara, A. E., Alawida, M., & Abiodun, O. I. (2023). Drone cybersecurity issues, solutions, trend insights and future perspectives: a survey. Neural computing and applications 2023; 35(31): 23063-23101, http://dx.doi.org/10.1007/s00521-023-08857-7.
- 44. Jakubowski R., Orkisz M., Wołoszyn T.: Identification of the electric brushless motor characteristics, in Scientific aspects of unmanned mobile vehicle, Kielce University of Technology, Kielce: 2010.
- 45. Budziłowicz, A. Zastosowanie Silników BLDC (ang. BrushLess Direct-Current motor) we współczesnych napędach elektrycznych i w motoryzacji. Autobusy: technika, eksploatacja, systemy transportowe 2015; 16(6): 49-52.
- 46. Maciejewska, M., Kardach, M., Galant, M., & Fuć, P. Analiza ryzyka zagrożeń w locie bezzałogowych statków powietrznych. Journal of KONBiN 2019; 49, http://dx.doi.org/10.2478/jok-2019-0062.

#### **Key Acronyms**

UAV	Unmanned aerial vehicle
ASRS	Aviation Safety Reporting System
MLE	Maximum Likelihood Estimation
LiPo	Lithium Polymer
ESC	Electronic Speed Controller
IMU	Inertial Measurement Unit
P	Positioning
S	Sport
T	Tripod
ATTI	Attitude
GNSS	Global Navigation Satellite System
GPS	Global Positioning System
BTS	Base transceiver station
GSM	Global System for Mobile Communicatio
AIC	Akaike Information Criterion

BIC Bayesian Information Criterion
MTTF Mean Time To Failure
MTBF Mean Time Between Failures